INTERNAL MODEL CONTROL FOR TRAJECTORY TRACKING OF AN OMNI-DIRECTIONAL ROBOT

Andrea Cassia Peixoto Bitencourt, andreabitencourt@yahoo.com.br
Alexandre da Costa e Silva Franco, acsfranco@yahoo.com.br
Marcelo Embiruçu de Souza, embirucu@ufba.br
Cristiano Hora de Oliveira Fontes, cfontes@ufba.br
Augusto Cesar Pinto Loureiro da Costa, augusto.loureiro@ufba.br
Programa de Pós-Graduação em Mecatrônica - Universidade Federal da Bahia
Rua Professor Aristides Novis, 2, Federação, Salvador - BA - Brasil. CEP: 40210-630

Abstract *Autonomous and semi-autonomous vehicles in non-structured and dynamical environments are the aims and scope of mobile robotics and, in such field, trajectory tracking control is an important issue. The objective of the present work is the design and application of a control structure able to cope with the problem of tracking arbitrary trajectories, which is a fundamental task for the high performance of such autonomous vehicles. The designed strategy was implemented and evaluated through simulation studies using Matlab. Moreover, kinematical and dynamic models of an omni-directional mobile robot, called as "Axebot", are presented. This robot has abilities for robot football competitions, such as those promoted by the RoboCup Federation (category F180). The control structure used for robot trajectory tracking control is based on the Internal Model Control (IMC). In this sense, an open-loop control scheme is designed, through inverse kinematical and dynamic models. This open-loop scheme is coupled with a feedback control structure, based on theoretic models of the robot. This feedback component allows the control strategy to cope with model mismatch and non-measured or non-modeled disturbances. The presented results shows that, in the absence of disturbances or modeling errors, the open-loop strategy based on inverse models is enough to accurate set-point tracking of specified trajectories. In the presence of external disturbances or modeling errors, the feedback block provides the necessary corrections to maintain the good behavior of the control system.*

Keywords: *Mobile robotics, Omni-directional Robot, Trajectory tracking Control*

1. INTRODUCTION

Mobile robotics is a field in robotic research that deals with the design and control of autonomous and semi-autonomous vehicles, with the propose of performing in structured, non-structured and dynamic enviroments. The autonomous mobile robots are generally characterized by the ability of making individual task, or in cooperation with others robots, without any or almost any human intervention. Autonomy and cooperation are characteristics that demand research in the artificial intelligence field, specially in the field of autonomous agents and multiagent systems.

Interests in autonomous mobile robots are mainly due to its autonomous moving features. Several researches have been developed in the area of the mobile robots covering interdisciplinary studies in mechanical and electrical engineering and computation. Techniques of artificial intelligence, modelling process control, computational algorithm, materials, nanotechnology and sensors fusion are examples of research that encompass several areas (Veloso, Stone et al. 1997; Watanabe 1998; Watanabe, Shiraishi et al. 1998; Brian, Matt et al. 2001; Young, Xiaofei et al. 2001; Kodagoda, Wijesoma et al. 2002; Albagul and Wahyudi 2004).

Mobile robots are tools of great usefulness for industrial and medical services and domestic tasks. Their usage is clearly growing in tasks that demand ability, safety and precision. Examples of such tasks are inspection of pipes in gas pipelines, intervention in kettles and oil wells, among others.

In this work an omni-directional mobile robot, called as Axebot, is modeled and controlled. This robot has abilities to execute autonomous tasks, such as the Robot Soccer Challenge. The Robot football challenge have been used as laboratory for researches developed in the fields of mobile robotics and artificial intelligence since 1996 (Franco and Costa 2006). The Robot Soccer demand, among other things, that the robot moves from a point to another as fast and accurate as possible. One of the necessary requirements to guarantee this ability is the availability of a trajectory tracking control system.

The control system uses robot sensors to obtain information and uses this information, together with some process knowledge, to manipulate robot actuators, in order to follow the desired trajectory. This work deals with the design and application of a control structure able to cope with the problem of tracking arbitrary trajectories for the Axebot robot. The objective is to make robot capable of following arbitrary trajectory, even in the presence of disturbances, such as the influence of the static friction, and model mismatch, which is a fundamental task for the high performance of such autonomous vehicles.

In section 2 we introduce the main characteristics of the mobile Axebot robot, and a brief description about the kinematical and dynamic models of the robot. Section 3 describes the main characteristics of the control structure used

in the trajectory control, based on the internal model control. Section 4 presents results and discussions. Conclusions and perspectives for futures works are presented in the last section.

2. AXEBOT MOBILE ROBOT

A mobile robot is a mechanical device mounted on a mobile base, that acts under the control of a computational system, equipped with sensors and actuators that allow it to interact with the environment (MarchiI 2001). The robot is able to move on the room, avoiding collisions against static or dynamic obstacles, in order to carry out their objectives.
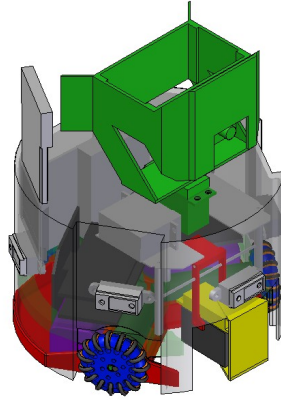

Figure 1. Axebot mobile robot

Figure 1 illustrates the mobile Axebot robot, an omni-directional robot with three omni-directional wheels disposed $120°$ among them. The wheels used in this kind of robot possess roller on the contact surface. These rollers reduce the attrition of lateral sliding of the wheel, resulting in one more degree of freedom to the wheel. This robot has the ability to move in any direction, without an orientation change.

Their kinematic and dynamic models are shown in the following. In this study, some assumptions were made, standing out the following: the robot is constituted of rigid material and any type of deformation is considered; there is only one point of contact of each wheel with the surface, and the velocities of these points are zero (i.e., it was not considered the sliding of the wheels).

2.1 kinematic Model

The kinematical model describes robot motion equations as a function of wheels velocities.

The AxeBot upper view and their coordinates systems is shown at Figure 2. Five coordinates reference systems were defined. Four of them are local reference systems, and the last one is an inertial reference system S_I. The local reference system S_R has its origin on the robot center of mass. The local reference system S_{Ci} is fastened in the wheel i $i = 1, 2, 3$. In figure 2, l is the distance between the centers of the coordinate systems S_I and S_{Ci}, ϕ_i is the wheel i inclination angle in the S_R system and θ is the robot orientation angle in the system S_I.

The position and the orientation of robot mass center in S_I coordinate system can be represented by

$$\xi_I = \begin{bmatrix} x_I \\ y_I \\ \theta \end{bmatrix} \tag{1}$$

where ξ_I represents robot posture vector (position and orientation); x_I and y_I are, respectively, robot position on x and y axes of S_I reference system; and θ is the orientation. The relationship between robot mass center velocity components on both S_I and S_R reference systems is:

$$\dot{\xi_I} = R^{-1}(\theta)\dot{\xi_R} \tag{2}$$

where $\dot{\xi_R}$ are robot mass center velocity components on S_R reference system, $\dot{\xi_I}$ are robot mass center velocity components on S_I reference system; and $R(\theta)$ is an orthogonal rotation matrix from S_R to S_I reference system given by:

$$R(\theta) = \begin{bmatrix} \cos(\theta) & -\sin(\theta) & 0 \\ \sin(\theta) & \cos(\theta) & 0 \\ 0 & 0 & 1 \end{bmatrix} \tag{3}$$
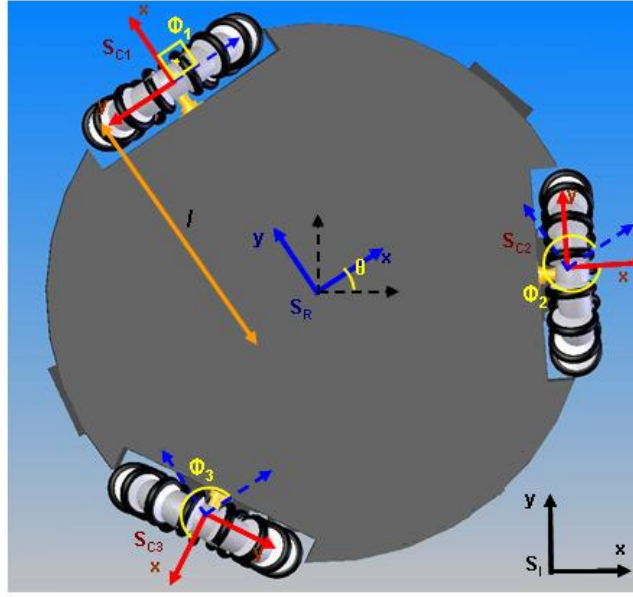
Figure 2. Geometry of Axebot and its coordinates systems

Robot mass center velocity components on S_R system are function of velocity components on S_{Ci} system. The relationship between these velocity components is

$$
\begin{bmatrix} v_{xR} \\ v_{yR} \\ \dot{\theta} \end{bmatrix} = \begin{bmatrix} \cos(\phi_i) & -\sin(\phi_i) & l\sin(\phi_i) \\ \sin(\phi_i) & \cos(\phi_i) & -l\cos(\phi_i) \\ 0 & 0 & 1 \end{bmatrix} \begin{bmatrix} v_{xCi} \\ v_{yCi} \\ \dot{\theta} \end{bmatrix}
\tag{4}
$$

Considering the kinematical restrictions of the omni-directional wheels used in AxeBot, and their disposition in the robot, where $\phi_1 = 90°$, $\phi_2 = 210°$ and $\phi_3 = 330°$, it was obtained the direct kinematical model of the robot, as follows:

$$
\begin{bmatrix} v_{xR} \\ v_{yR} \\ \dot{\theta} \end{bmatrix} = R \begin{bmatrix} -\frac{2}{3} & \frac{1}{3} & \frac{1}{3} \\ 0 & \frac{1}{\sqrt{3}} & -\frac{1}{\sqrt{3}} \\ \frac{1}{3l} & \frac{1}{3l} & \frac{1}{3l} \end{bmatrix} \begin{bmatrix} \dot{\varphi}_{1x} \\ \dot{\varphi}_{2x} \\ \dot{\varphi}_{3x} \end{bmatrix}
\tag{5}
$$

where φ_{ix} is wheel i angular velocity relative to x axis of S_{Ci} system and R is the distance between wheel extremity and its center. Applying the transformation of S_R local coordinate system into inertial one, the relationship of robot velocity in the inertial system as a function of wheels angular velocities is

$$
\begin{bmatrix} v_{xI} \\ v_{yI} \\ \dot{\theta} \end{bmatrix} = R \begin{bmatrix} -\frac{2\cos(\theta)}{3} & \frac{\sqrt{3}\cos(\theta)-3\sin(\theta)}{3\sqrt{3}} & \frac{\sqrt{3}\cos(\theta)+3\sin(\theta)}{3\sqrt{3}} \\ -\frac{2\sin(\theta)}{3} & \frac{\sqrt{3}\sin(\theta)+3\cos(\theta)}{3\sqrt{3}} & \frac{\sqrt{3}\sin(\theta)-3\cos(\theta)}{3\sqrt{3}} \\ \frac{1}{3l} & \frac{1}{3l} & \frac{1}{3l} \end{bmatrix} \begin{bmatrix} \dot{\varphi}_{1x} \\ \dot{\varphi}_{2x} \\ \dot{\varphi}_{3x} \end{bmatrix}
\tag{6}
$$

2.2 Dynamic Model

The dynamic model describes robot motion equations considering the forces that act itself. Initially this section presents the dynamic model of AxeBot mobile base, without explicitly considering the torque generated by actuators. Further actuators dynamic models are presented, taking into account mechanical and electric aspects. Finally, the complete dynamic model of AxeBot is shown, resulting from the joint equations of mobile base model and actuators models.

Motions of a rigid body are caused by external forces that act at the body. These motions can be classified into translation and rotation motions. The dynamic model of AxeBot was formulated according to Newton's laws:

$$
\sum F = m.a
\tag{7}
$$

$$
\sum M_o = I_z.\ddot{\theta}
\tag{8}
$$

where F are forces which act on the robot, m is mass, a is acceleration, M_o is angular momentum, I_z is inertia momentum and $\ddot{\theta}$ is angular acceleration.
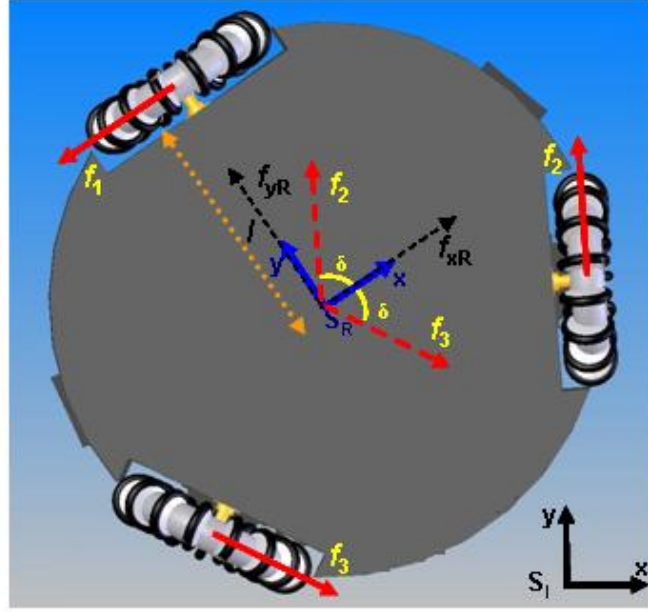

Figure 3. Forces acting at the body.

The Figure 3 shows an upper view of AxeBot, with some aspects of its geometry and traction forces f_1, f_2 and f_3 acting on wheels 1, 2 and 3, respectively. Components of robot mass center resultant force, f_{xR} and f_{yR}, are projections of this force on S_R system. δ is the angle formed between S_R system x axis and forces f_2 and f_3. Through eqs. (7) and (8) and considering the forces acting in the robot, one can observe the following relationships:

$$f_{xI} = ma_{xI} \tag{9}$$

$$f_{yI} = ma_{yI} \tag{10}$$

$$\sum M_o = f_1 l + f_2 l + f_3 l = J_r \ddot{\theta} \tag{11}$$

where $\sum M_o$ is the resultant momentum of forces f_1, f_2 and f_3 on robot mass center, J_r is the inertia moment on z axis of S_R system, f_{xI} and f_{yI} are projections of resultant force components on S_I inertial system, m is the robot mass and a_{xI} and a_{yI} are their acceleration components in S_I system,

$$F_I = R^{-1}(\theta) F_R \tag{12}$$

$$\ddot{\xi}_I = R^{-1}(\theta)\ddot{\xi}_R + R^{-1}(\dot{\theta})\dot{\xi}_R \tag{13}$$

where $F_I = \begin{bmatrix} f_{xI} & f_{yI} & \sum M_o \end{bmatrix}^T$, $F_R = \begin{bmatrix} f_{xR} & f_{yR} & \sum M_o \end{bmatrix}^T$ and $R^{-1}(\dot{\theta})$ is the Jacobian of the inverse matrix $R(\theta)$. Substituting eqs. (12) and (13) into eqs. (9) and (10), we obtain

$$f_{xR} = m(a_{xR} - v_{yR}\dot{\theta}) \tag{14}$$

$$f_{yR} = m(a_{yR} + v_{xR}\dot{\theta}) \tag{15}$$

Writing f_{xR} and f_{yR} as functions of f_1, f_2 and f_3,

$$f_{xR} = -f_1 + f_2 \cos\delta + f_3 \cos\delta \tag{16}$$

$$f_{yR} = f_2 \sin\delta + f_3 \sin\delta \tag{17}$$

Substituting eqs. (16) and (17) into eqs. (14) and (15), and isolating acceleration components, we can obtain the dynamic model of robot mobile base:

$$a_{xR} = \frac{-f_1 + f_2 \cos\delta + f_3 \cos\delta}{m} + v_{yR}\dot{\theta} \tag{18}$$

$$a_{yR} = \frac{f_2 \sin\delta - f_3 \sin\delta}{m} - v_{xR}\dot\theta \tag{19}$$

$$\ddot\theta = \frac{f_1 l + f_2 l + f_3 l}{J_r} \tag{20}$$

Axebot actuation system is composed by three continuous current motors coupled in a 19:1 reduction box (Franco and Costa 2006) (see fig.4)).

Figure 4. Maxon Motor, Amax 22 R179-6V model.

The dynamic model of a continuous current motor (DC motor) is formulated considering their mechanical and electric aspects. The dynamic equations of a DC motor can be expressed by the electric part:

$$u_i = L_a \frac{di_{a_i}}{dt} + R_a i_{a_i} + e_i \tag{21}$$

and by the mechanical one:

$$\tau_i = J_m \dot\omega_{m_i} + B_{vis}\omega_{m_i} + \frac{Rf_i}{\kappa n} \tag{22}$$

where L_a and R_a are, respectively, motors inductance and resistance, J_m and B_{vis} are, respectively, inertia moment and viscous attrition constant of the mechanical part of the actuators, and u_i, i_{a_i}, τ_i, ω_{m_i}, f_i and n are, respectively, entrance tension, armor current, torque, velocity of wheel i motor, wheel i traction force and reduction factor of reduction box and k is coupling efficiency degree. Motor torque is directly proportional to its armor current and contra-electrometric force is proportional to angular velocity:

$$\tau_i = k_T i_{a_i} \tag{23}$$

$$e_i = k_{em}\omega_{m_i} \tag{24}$$

where k_T and K_{em} are torque and contra-electrometric constants, respectively.
Relating u_i as a function of τ_i,

$$u_i = L_a \frac{\dot\tau_i}{k_T} + R_a \frac{\tau_i}{k_T} + k_{em}\omega_{m_i} \tag{25}$$

Substituting the values of τ_i and $\dot\tau_i$ from eq.(22) into eq. (25) we obtain

$$u_i = \frac{L_a J_m}{k_T}\ddot\omega_{m_i} + (\frac{R_a J_m + L_a B_{vis}}{k_T})\dot\omega_{m_i} + (\frac{R_a B_{vis} + k_T k_{em}}{k_T})\omega_{m_i} + \frac{R_a f_i R}{\kappa n k_T} + \frac{L_a \dot f_i R}{\kappa n k_T} \tag{26}$$

The expression above relates motor angular velocity as a function of its entrance tension. However, motors are activated by a pulse width λ_i that generates the entrance tension u_i of the motor i as a function of an average reference tension V_{ref} . The pulse width is

$$\lambda_i = \frac{u_i}{V_{ref}} \tag{27}$$

Substituting eq. (27) into eq. (26), actuator dynamics will have the following pulse width as input:

$$\lambda_i = \frac{L_a J_m}{k_T V_{ref}} \ddot{\omega}_{m_i} + (\frac{R_a J_m + L_a B_{vis}}{k_T V_{ref}}) \dot{\omega}_{m_i} + (\frac{R_a B_{vis} + k_T k_{em}}{k_T V_{ref}}) \omega_{m_i} + \frac{R_a f_i R}{n \kappa k_T V_{ref}} + \frac{L_a \dot{f}_i R}{n \kappa k_T V_{ref}} \tag{28}$$

Isolating f_i forces from eqs. (18), (19) and (20) and substituting into eq. (28), using eq.(5) and its derivatives, we obtain the equations of robot mobile base inverse dynamics, including also actuator eqs. (29 - 31),

$$\begin{aligned} \lambda_1 = \ & \beta_{i2} \ddot{\omega}_{m_1} + \beta_{i3} \ddot{\omega}_{m_2} + \beta_{i3} \ddot{\omega}_{m_3} + (\beta_{i4} + \beta_{i5} \omega_{m_2} - \beta_{i5} \omega_{m_3}) \dot{\omega}_{m_1} + (\beta_{i6} + 2\beta_{i5} \omega_{m_2} + \beta_{i5} \omega_{m_1}) \dot{\omega}_{m_2} \\ & + (\beta_{i6} - \beta_{i5} \omega_{m_1} - 2\beta_{i5} \omega_{m_3}) \dot{\omega}_{m_3} + (\beta_{i7} + \beta_{i8} \omega_{m_2} - \beta_{i8} \omega_{m_3}) \omega_{m_1} + (\beta_{i8} \omega_{m_2}) \omega_{m_2} + (-\beta_{i8} \omega_{m_3}) \omega_{m_3} \end{aligned} \tag{29}$$

$$\begin{aligned} \lambda_2 = \ & \beta_{i3} \ddot{\omega}_{m_1} + \beta_{i2} \ddot{\omega}_{m_2} + \beta_{i3} \ddot{\omega}_{m_3} + (\beta_{i6} - 2\beta_{i5} \omega_{m_1} + \beta_{i5} \omega_{m_2}) \dot{\omega}_{m_1} + (\beta_{i4} - \beta_{i5} \omega_{m_1} + \beta_{i5} \omega_{m_2}) \dot{\omega}_{m_2} \\ & + (\beta_{i6} + \beta_{i5} \omega_{m_2} + 2\beta_{i5} \omega_{m_3}) \dot{\omega}_{m_3} + (-\beta_{i8} \omega_{m_1} - \beta_{i8} \omega_{m_2}) \omega_{m_1} + (\beta_{i7} + \beta_{i8} \omega_{m_3}) \omega_{m_2} + (\beta_{i8} \omega_{m_3}) \omega_{m_3} \end{aligned} \tag{30}$$

$$\begin{aligned} \lambda_3 = \ & \beta_{i3} \ddot{\omega}_{m_1} + \beta_{i3} \ddot{\omega}_{m_2} + \beta_{i2} \ddot{\omega}_{m_3} + (\beta_{i6} - 2\beta_{i5} \omega_{m_1} + \beta_{i5} \omega_{m_3}) \dot{\omega}_{m_1} + (\beta_{i6} - 2\beta_{i5} \omega_{m_2} - \beta_{i5} \omega_{m_3}) \dot{\omega}_{m_2} \\ & + (\beta_{i4} + \beta_{i5} \omega_{m_1} - \beta_{i5} \omega_{m_2}) \dot{\omega}_{m_3} + (\beta_{i8} \omega_{m_1} + \beta_{i8} \omega_{m_3}) \omega_{m_1} + (-\beta_{i8} \omega_{m_2} - \beta_{i8} \omega_{m_3}) \omega_{m_2} + \beta_{i7} \omega_{m_3} \end{aligned} \tag{31}$$

where

$$\begin{aligned} \beta_{i1} = \ & 1/(27 n^3 l^2 \kappa k_T V_{ref}) \\ \beta_{i2} = \ & (3 L_a R^2 J_r n + 12 L_a R^2 m l^2 n + 27 L_a J_m l^2 \kappa n^3) \beta_{i1} \\ \beta_{i3} = \ & (-6 L_a R^2 m l^2 n + 3 L_a R^2 J_r n) \beta_{i1} \\ \beta_{i4} = \ & (12 R_a R^2 m l^2 n + 27 l^2 \kappa n^3 L_a B_{vis} + 27 l^2 \kappa n^3 R_a J_m + 3 R_a R^2 J_r n) \beta_{i1} \\ \beta_{i5} = \ & (2 L_a R^3 \sqrt{3} m l) \beta_{i1} \\ \beta_{i6} = \ & (-6 R_a R^2 m l^2 n + 3 R_a R^2 J_r n) \beta_{i1} \\ \beta_{i7} = \ & (27 l^2 \kappa n^3 k_{em} + 27 l^2 \kappa n^3 R_a B_{vis}) \beta_{i1} \\ \beta_{i8} = \ & (2 R_a R^3 \sqrt{3} m l) \beta_{i1} \end{aligned}$$

Getting motor angular acceleration derivative components from eqs. (29 - 31), we obtain the final equations of the dynamics of robot mobile base :

$$\begin{aligned} \ddot{\omega}_{m_1} = \ & \beta_{d2} \lambda_1 + \beta_{d3} \lambda_2 + \beta_{d3} \lambda_3 + (\beta_{d4} + \beta_{d5} \omega_{m_2} - \beta_{d5} \omega_{m_3}) \dot{\omega}_{m_1} + (\beta_{d6} + 2\beta_{d5} \omega_{m_2} \\ & + \beta_{d5} \omega_{m_1}) \dot{\omega}_{m_2} + (\beta_{d6} - \beta_{d5} \omega_{m_1} - 2\beta_{d5} \omega_{m_3}) \dot{\omega}_{m_3} + (\beta_{d7} + \beta_{d8} \omega_{m_2} - \beta_{d8} \omega_{m_3}) \omega_{m_1} \\ & + (\beta_{d9} + \beta_{d8} \omega_{m_2}) \omega_{m_2} + (\beta_{d9} - \beta_{d8} \omega_{m_3}) \omega_{m_3} \end{aligned} \tag{32}$$

$$\begin{aligned} \ddot{\omega}_{m_2} = \ & \beta_{d3} \lambda_1 + \beta_{d2} \lambda_2 + \beta_{d3} \lambda_3 + (\beta_{d6} - 2\beta_{d5} \omega_{m_1} + \beta_{d5} \omega_{m_2}) \dot{\omega}_{m_1} + (\beta_{d4} - \beta_{d5} \omega_{m_1} \\ & + \beta_{d5} \omega_{m_2}) \dot{\omega}_{m_2} + (\beta_{d6} + \beta_{d5} \omega_{m_2} + 2\beta_{d5} \omega_{m_3}) \dot{\omega}_{m_3} + (\beta_{d9} - \beta_{d8} \omega_{m_1} - \beta_{d8} \omega_{m_2}) \omega_{m_1} \\ & + (\beta_{d7} + \beta_{d8} \omega_{m_3}) \omega_{m_2} + (\beta_{d9} + \beta_{d8} \omega_{m_3}) \omega_{m_3} \end{aligned} \tag{33}$$

$$\begin{aligned} \ddot{\omega}_{m_3} = \ & \beta_{d3} \lambda_1 + \beta_{d3} \lambda_2 + \beta_{d2} \lambda_3 + (\beta_{d6} - 2\beta_{d5} \omega_{m_1} + \beta_{d5} \omega_{m_3}) \dot{\omega}_{m_1} + (\beta_{d6} - 2\beta_{d5} \omega_{m_2} \\ & - \beta_{d5} \omega_{m_3}) \dot{\omega}_{m_2} + (\beta_{d4} + \beta_{d5} \omega_{m_1} - \beta_{d5} \omega_{m_2}) \dot{\omega}_{m_3} + (\beta_{d9} + \beta_{d8} \omega_{m_1} + \beta_{d8} \omega_{m_3}) \omega_{m_1} \\ & + (\beta_{d9} - \beta_{d8} \omega_{m_2} - \beta_{d8} \omega_{m_3}) \omega_{m_2} + \beta_{d7} \omega_{m_3} \end{aligned} \tag{34}$$

where

$$\begin{aligned} \beta_{d1} = \ & -1/9/l/n/(9 J_m^2 l^2 \kappa^2 n^4 + 3 R^2 J_r J_m \kappa n^2 + 6 R^2 m l^2 J_m \kappa n^2 + 2 R^4 J_r m)/L_a \\ \beta_{d2} = \ & -81 V_{ref} k_T \kappa^2 n^5 l^3 J_m - 18 V_{ref} k_T \kappa n^3 R^2 l^3 m - 18 V_{ref} k_T \kappa n^3 R^2 l J_r \\ \beta_{d3} = \ & 9 V_{ref} k_T \kappa n^3 l R^2 J_r - 18 V_{ref} k_T \kappa n^3 l^3 R^2 m \\ \beta_{d4} = \ & 27 J_m l \kappa n^3 R_a R^2 J_r + 54 J_m l^3 \kappa n^3 R_a R^2 m + 81 J_m l^3 \kappa^2 n^5 L_a B_{vis} + 81 J_m^2 l^3 \kappa^2 n^5 R_a \\ & + 18 R^4 J_r R_a m l n + 18 R^2 m l^3 \kappa n^3 L_a B_{vis} + 18 R^2 J_r l \kappa n^3 L_a B_{vis} \\ \beta_{d5} = \ & 2 R^5 J_r L_a \sqrt{3} m + 6 J_m l^2 \kappa n^2 L_a R^3 \sqrt{3} m \\ \beta_{d6} = \ & +18 R^2 m l^3 \kappa n^3 L_a B_{vis} - 9 R^2 J_r l \kappa n^3 L_a B_{vis} \end{aligned}$$

$$\beta_{d7} = 81J_m l^3 \kappa^2 n^5 R_a B_{vis} + 81J_m l^3 \kappa^2 n^5 k_{em} k_T + 18R^2 J_r l\kappa n^3 k_{em} k_T$$
$$+18R^2 J_r l\kappa n^3 R_a B_{vis} + 18R^2 m l^3 \kappa n^3 k_{em} k_T + 18R^2 m l^3 \kappa n^3 R_a B_{vis}$$
$$\beta_{d8} = 2R^5 J_r R_a \sqrt{3} m + 6J_m l^2 \kappa n^2 R_a R^3 \sqrt{3} m$$
$$\beta_{d9} = +18R^2 m l^3 \kappa n^3 R_a B_{vis} + 18R^2 m l^3 \kappa n^3 k_{em} k_T - 9R^2 J_r l\kappa n^3 k_{em} k_T$$
$$-9R^2 J_r l\kappa n^3 R_a B_{vis}$$

In eqs. (29 - 31) values of wheels angular velocity,$\dot{\varphi}_{ix}$, were substituted by motors angular velocity values,ω_{m_i} , using $\dot{\varphi}_{ix} = \frac{\omega_{m_i}}{n}$.

The Axebot parameters and their values are given in Tab. 1.

Table 1. Axebot parameters.

Parameter	Value	Unit
m	$3,4$	$[kg]$
J_r	$2,125$	$[kgm^2]$
l	$0,09$	$[m]$
R	$0,024$	$[m]$
L_a	$0,00011$	$[H]$
R_a	$1,71$	$[Ohm]$
n	$19{:}1$	-
J_m	$3,88 \times 10^{-7}$	$[kgm^2]$
K_{em}	$0,0059$	$[Volts/rad]$
K_t	$0,0059$	$[Nm/A]$
B_{vis}	$2,4 \times 10^{-6}$	$[Nms/rad]$
V_d	6	$[Volt]$

3. Trajectory Controller

The trajectory control objective is to position the robot on a previously defined track, characterizing a servo problem control with variable set-point. The mobile robots trajectory control can be split in three types: control considering only the kinematical model, control considering only the dynamic model and control using both the kinematical and dynamic models (Sousa and Hemerly 2003). This work presents a control scheme in closed-loop, composed of a cascade controller, where the master controller is based on the kinematical control, to track the reference posture, generating reference velocities to the internal control-loop which determines the reference pulse width through the knowledge of robot theoretical model. This structure is called Internal Model Control(IMC).

The IMC controller is capable of estimate and correct robot model mismatch and unmeasured disturbances. The block diagram of the control system proposed in this work is presented in fig.5.
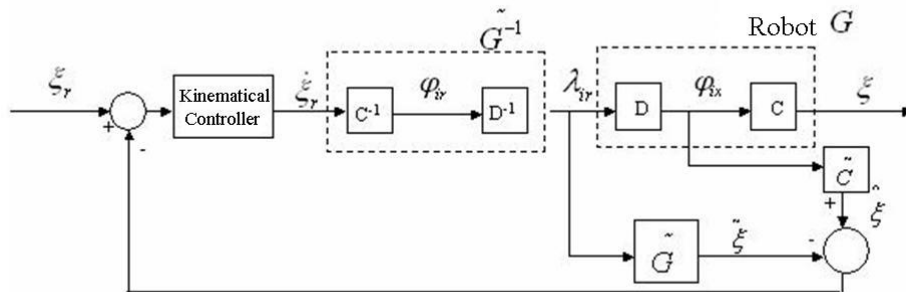

Figure 5. Blocks diagram of the control system.

In figure 5, C e D are AxeBot kinematical and dynamic models, respectively. ξ_r, $\dot{\xi}_r$, φ_{ir}, λ_{ir}, φ_{ix}, ξ, $\hat{\xi}$, $\tilde{\xi}$ are, respectively, the set-point posture of the robot, the set-point velocity of the robot, the set-point angular velocity of the wheels, the set-point pulse width, the measured angular velocity of the wheels, the posture of the robot, and the inferred and calculated posture from the theoretical model. G, $\tilde{G}$ and G^{-1} are, respectively, the real robot, the theoretical model of the robot and the inverse theoretical model.

3.1 Control based on the Kinematic

The control based on the kinematical model generates the components of robot set-point velocity ($\dot{\xi}_r$), relative to local reference coordinates system, as a function of posture error ($\Delta\xi_r$). The control law for the kinematical controller can be represented by

$$\dot{\xi}_{R_r} = (\xi_{I_r} - \xi_I)R(\theta)K \tag{35}$$

where $\dot{\xi}_{R_r}$ is robot set-point velocity relative to local reference coordinates system, ξ_{I_r} is posture set-point, ξ_I is robot posture, $R(\theta)$ is the transformation matrix from the inertial reference system to local one, represented by eq. (3), and K is a diagonal matrix of positive constants.

3.2 CONTROLLER IMC

The IMC (Internal Model Control) control structure was introduced by Garcia and Morari in 1982 (Lee, T. et al. 1993). The controller equation is developed from the knowledge of a model of the robot. This control structure was used in an open-loop scheme coupled with a feedback control structure in cascade with the kinematical controller.

For this controller robot kinematical and dynamic models, and also their inverse models, are used.

The equation of the inverse kinematical model is found getting wheels angular speed components from eq.(6). Therefore, we can generate the equation which determine wheel angular speed from robot mobile base speed,

$$\begin{bmatrix} \dot{\varphi_{1x}} \\ \dot{\varphi_{2x}} \\ \dot{\varphi_{3x}} \end{bmatrix} = \frac{1}{R} \begin{bmatrix} -\cos(\theta) & -\sin(\theta) & l \\ \frac{\cos(\theta)-\sqrt{3}\sin(\theta)}{2} & \frac{\sin(\theta)+\sqrt{3}\cos(\theta)}{2} & l \\ \frac{\cos(\theta)+\sqrt{3}\sin(\theta)}{2} & \frac{\sin(\theta)-\sqrt{3}\cos(\theta)}{2} & l \end{bmatrix} \begin{bmatrix} v_{xI} \\ v_{yI} \\ \dot{\theta} \end{bmatrix} \tag{36}$$

Dynamic inverse model equation, represented by eqs.(29) through (31) determines the pulse width that should be applied in wheel motors, using wheels angular speed set-point supplied by inverse kinematical model.

In a first approach a controller was developed in an open-loop scheme. This approach may present satisfactory results in the absence of disturbances and model mismatch. When coping with modeling errors, a current feature of real systems , performance may deteriorate, and robot behavior may even gets unstable.

In a second approach the open-loop scheme was coupled with the feedback control structure. This feedback component allows the whole control scheme to be able to cope with model mismatch and non-measured or non-modeled disturbances. This configuration can be interpreted as a combination of open-loop and closed-loop configurations, and provides the advantages of both structures.

4. RESULTS AND DISCUSSION

The analysis of the controller performance was accomplished in two stages. In the first one, control system was analyzed in an open-loop scheme in the absence of model mismatch or non-measured or non-modeled disturbances. For this situation, the controller without feedback performs very well as shown in fig. 6. This figure shows a good behavior of the control system in tracking the desired robot trajectory.
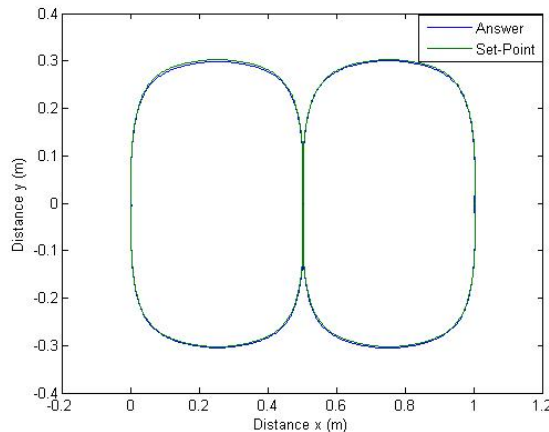

Figure 6. System response with open-loop control scheme.

In the second stage, errors on model parameters was included and a dead zone non-linearity. For instance, this disturbance may represent static attrition3. In this situation, the open-loop scheme has its performance greatly degraded. On the other hand, adding the feedback structure allows a significant improvement and an effective control of robot trajectory, which can be verified in fig. 7.
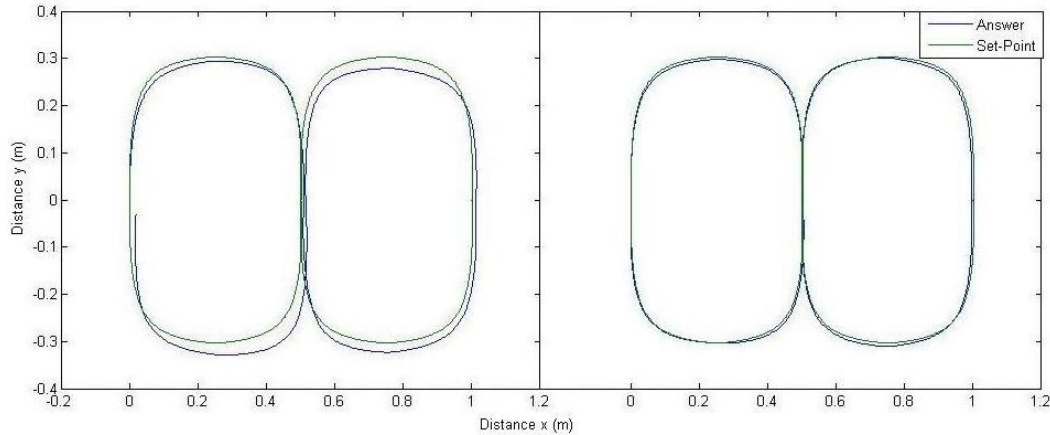

Figure 7. Response with with open-loop (left) and closed-loop (right) schemes, under non-modeled disturbances.

For comparison of controllers performance, ISE (Integral of Squared Error) performance index was used eq. (37).

$$I = \int\limits_{t=0}^{T} \mathbf{e}^T \mathbf{e} dt \qquad (37)$$

where I is the ISE performance index, T is the integration time and $\mathbf{e}$ is the error vector.

The ISE value obtained in the open-loop scheme was 0.61 for position and 20.6928 for speed. With the inclusion of feedback there was a substantial reduction of these values: for the position ISE was 0.0706 and for speed ISE was 1.7745.

5. CONCLUSIONS

This work presents a study on the trajectory control of an omni-directional mobile robot. We have presented the physical, mechanical and electric characteristics of the robot, through their kinematical and dynamic models. In the first stage of the work a controller was implemented in an open-loop scheme, presenting satisfactory results in the absence of noises and disturbances. In order to improve the controller performance in the presence of noises and modeling errors, a feedback structure was added with the objective of estimating and compensating for the effects of such disturbances. The evaluation of controllers performances may be observed both through graphical inspection of robot trajectory as well as by the ISE value. The comparative analysis of ISE values for position presents a reduction of 88% after joining the feedback control structure, and a reduction of 91% for speed. In further works a control system for trajectory tracking for omni-directional robots with tolerance to wheels sliding will be developed. This is a very common disturbance in wheels mobile robots.

6. ACKNOWLEDGEMENTS

7. REFERENCES

Albagul, A. and Wahyudi 2004."Dynamic Modelling and Adaptive Traction Control for Mobile Robots." International Journal of Advanced Robotic Systems, Vol. 1, No 3, pp. 149-154

Brian, C., G. Matt, et al. (2001). Mechanical Design and Modeling of an Omni-directional RoboCup Player. , Department of Mechanical Engineering an Innovation in Mechanics and Management, Ohio University and University of Padova.

Franco, A. and A. L. Costa (2006). "Modelagem e simulação do robô omni-direcional AxeBot." CBA.

Kodagoda, K. R. S., W. S. Wijesoma, et al. (2002). "Fuzzy Speed and Steering Control of an AGV." IEEE Transactions on control systems technology 10(1): 112-120.

Lee, T. H., S. L. T., et al. (1993). "Internal Model Control (IMC)." Approach for Designing Disk Drive Servo-Controller: 2024-2027.

MarchiI, J. (2001). Navegacão de robôs móveis autônomos: Estudo e implementação de abordagens, UFSC - Universidade Federal de Santa Catarina.

Sousa, C. and E. Hemerly (2003). "Controle de robôs moveis utilizando o modelo cinemático" Revista Controle $\&$ Automação 14(4): 384-392.

Veloso, M., P. Stone, et al. (1997). The CMUnited-97 Robotic Soccer Team: Perception and Multiagent Control. USA, Carnegie Mellon University.

Watanabe, K. (1998). "Control of an Omnidirectional Moblie Robot." IEEE Second International Conference on Knowledge Based Intelligent Electronics Systems: 51-60.

Watanabe, K., Y. Shiraishi, et al. (1998). "Feedback Control of Omnidirectional Autonomous Platform for Mobile Service Robots." Journal of Intelligent and Robotic System 22: 315-330

Young, L., W. Xiaofei, et al. (2001). "Omni-Directional Mobile Robot Controller Design by Trajectory Linearization." School of Electrical Engineering and Computer Science, Ohio University.

8. Responsibility notice

The author(s) is (are) the only responsible for the printed material included in this paper